Radiation Physics and Chemistry 208 (2023) 110933

Contents lists available at ScienceDirect

Radiation Physics and Chemistry

journal homepage: www.elsevier.com/locate/radphyschem

Systematic study of (p, n) and (p, 2n) reactions on ^{110}Cd

Vibhuti Vashi [a], Rajnikant Makwana [a,b,*], B. Quintana [b], M.H. Mehta [c], R.K. Singh [a], B.K. Soni [a], R. Chauhan [a], S. Mukherjee [a], M. Abhangi [c], S. Vala [c], N.L. Singh [a], G.B. Patel [a], S.V. Suryanarayana [d], B.K. Nayak [e], S.C. Sharma [f], T.N. Nag [g], Y. Kavun [h]

[a] Department of Physics, Faculty of Science, The Maharaja Sayajirao University of Baroda, Vadodara 390002, India
[b] Departamento de Física Fundamental, Universidad de Salamanca, Calle Espejo s/n, Salmanca 37007, Spain
[c] Institute for Plasma Research, Gandhinagar, Gujarat 382428, India
[d] Manipal Centre for Natural Sciences, MAHE, Manipal 576014, India
[e] Homi Bhabha National Institute, Anushaktinagar, Mumbai 400094, India
[f] Nuclear Physics Division, Bhabha Atomic Research Centre, Mumbai 400085, India
[g] Radiochemistry Division, Bhabha Atomic Research Centre, Mumbai 400085, India
[h] Kahramanmaras Sutcu Imam University, Vocational School of Health Services Dept. of Medical Imaging Tech., Kahramanmaras, Turkey

ARTICLE INFO

Keywords:
Nuclear reaction
Activation analysis
HPGe detector
Cadmium
γ-ray spectroscopy
Cross section

ABSTRACT

Standard activation analysis technique with γ ray spectroscopy via off-line mode was utilized for reaction cross section estimation. The proton beam was transported from the BARC-TIFR accelerator and targeted on the ^{nat}Cd target. The 16 MeV proton beam irradiated the sample, and Copper foil was utilized as an energy degrader. The activation cross sections were estimated for ^{110}Cd(p, n) reaction for the ground state ($J^{\pi} = 7^{+}$) population of ^{110}In nucleus and ^{110}Cd(p, 2n)^{109}In reaction at 14.14 MeV of proton energy. Along with experimental measurements, the theoretical study has been carried out for ground and metastable states population by utilizing the nuclear model code TALYS-1.95, EMPIRE-3.2.3, and ALICE-2014 for both reaction channels. The estimated cross sections are valuable for the improvement of theoretical nuclear model codes for a comprehensive knowledge of nuclear reaction mechanisms. The produced isotopes ^{109,110}In have significant importance in Positron Emission Tomography (PET) studies. The present study is a dive into the phenomenological and microscopic level density models of different nuclear model codes in predicting excitation functions.

1. Introduction

The experimental study on proton induced nuclear data are stimulated to improve the theoretical modeling for fundamental and applied research. Nuclear data related to the reactions produced using proton beam have many applications in nuclear reactors and technology, accelerator physics, cyclotrons, nuclear medicines, nuclear astrophysics to understand the driving mechanism behind the origin of the chemical elements, test the nuclear theories, and many more (Alhassan et al., 2020; Khandaker et al., 2014; Al-Abyad, 2012). The information of proton-generated nuclear data at intermediate energy has prime importance in the nuclear medicine and industrial sectors. On the contrary, high-energy single charged particle induced reactions are important for the advanced reactors for the generation of neutrons, too. In advanced nuclear reactors, high-energy proton beams interact with heavy target nuclei for the production of neutrons by spallation reactions. These spallation neutrons are capable of annihilating the nuclear waste and producing energy (Chadwik et al., 1999; Rubbia et al., 1995; Eyyup TEL et al., 2010).

However, Cadmium is a naturally occurring silver-white, soft, and ductile, it is a tarnishable metal. It is nearly divalent, and the chemical properties resemble zinc that is found in the earth's crust with a very common impurity of zinc ores (Cotton and Wilkinson, 1972). Due to the high neutron absorption capability of Cadmium, it is widely utilized as a control rod to control nuclear fission inside nuclear reactors (Mahmoud et al., 2020). The interaction of the recoil proton with Cd isotopes may transform them into other isotopes, and can change the characteristic of the controlling materials in reactors (Petti, 1989; Mongelli et al., 2005). Different concentration of CdO along with Bismuth Borate glasses is an excellent shielding material to shield gamma rays in various medical and industrial sectors (Alajerami et al., 2020). Besides applications in nuclear sciences and technology, Cadmium is also extensively used for many industrial purposes such

* Corresponding author at: Department of Physics, Faculty of Science, The Maharaja Sayajirao University of Baroda, Vadodara 390002, India.
E-mail address: r.j.makwana-phy@msubaroda.ac.in (R. Makwana).

https://doi.org/10.1016/j.radphyschem.2023.110933
Received 1 August 2022; Received in revised form 11 March 2023; Accepted 17 March 2023
Available online 21 March 2023
0969-806X/© 2023 Elsevier Ltd. All rights reserved.

as bearing alloys, galvanization, electroplating, manufacturing batteries and pigments (Rios and Méndez-Armenta, 2019; Tàrkànyi et al., 2006; Ali et al., 2014). Further, the cross section measurement of natural Cadmium is important for the procreation of experimental measurements with enriched targets as it contains all-natural elements with different ratios, and generated radionuclide contaminate the final product nuclides (Ditrói et al., 2016; Al-Saleh, 2008).

The estimation of cross sections for ^{110}Cd(p, n)^{110}In, and ^{110}Cd(p, 2n)^{109}In reactions has significant importance as proton irradiation on ^{110}Cd has many applications in thin layer activation analysis (TLA), medical isotope production, radioactive waste handling, etc. (Al-Abyad, 2012; Tàrkànyi et al., 2006; Al-Saleh, 2008). The half-life of ^{109,110}In product nuclei is 4.167 h and 4.92 h, respectively. As the product nuclei have a short half-life, these nuclei are convenient for PET studies (Al-Saleh, 2008). One of the significant applications of our proton induced reaction cross section with Cadmium target is to verify the theoretical codes and enhance the EXFOR database (Zerkin and Pritychenko, 2018).

The cross section ratio has significant importance for the nuclear model examination and to get a detailed understanding of the mechanism behind compound nuclear reactions (Patronis et al., 2007). The ratio of the ground state (σ_g) to metastable state (σ_m) depends on the spin of the states and the distribution of the compound nucleus (CN) that populated them (Georgali et al., 2020). The cross section ratio (σ_g/σ_m) has been studied for ^{110}Cd(p, n) reaction as it populates two levels of ^{110}In product nuclei, the ground state (7^+) and metastable (2^+) spin, that offers great sensitivity to analyze the angular distribution of the product nuclei (Patronis et al., 2007).

A detailed literature survey was carried out for ^{110}Cd(p, n)^{110}In (Otozai et al., 1966; Skakun et al., 1975a; Abramovich et al., 1975; Blaser et al., 1951), and ^{110}Cd(p, 2n)^{109}In (Otozai et al., 1966; Skakun et al., 1975a) reactions and it is found that the experimental data are insufficient. Hence, the goal of our study is to report the experimentally measured cross section data for both the reactions at 14.14 ± 2.03 MeV of proton energy. The estimated cross section data are simulated with the phenomenological and microscopic nuclear level densities (NLDs) of TALYS (v. 1.95) (Koning et al., 2017), EMPIRE (v. 3.2.3) (Herman et al., 2015), and ALICE-2014 (Blann, 1971) codes, and with the literature data collected from the EXFOR (Zerkin and Pritychenko, 2018). Further, theoretical calculations were carried out for ^{110}Cd(p, n)^{110m}In, and ^{110}Cd(p, n)^{110}In reactions using TALYS, EMPIRE, and ALICE codes. The theoretical study has been carried out to calculate cross section ratio of ^{110}Cd(p, n) reaction.

The irradiation experiment details, data analysis, and nuclear model codes utilized to carry out this work is given in the following sections. The cross section results along with previously reported data, available data libraries, and with theoretical calculations are presented in Section 5.

2. Irradiation experiment

The 16 MeV of proton beam was delivered from the BARC-TIFR accelerator facility at TIFR campus for the irradiation experiment. The proton beam was allowed to incident on the natural Cadmium target of ≈ 250-micron thickness followed by Copper degrader of ≈ 3.56 μm, and wrapped with Aluminum foil. The proton energy degradation was computed by utilizing MCNP code (ver. 6.2) (Werner, 2017) and plotted in Fig. 1. It is assumed that the reactions are taking place at the middle of the target, the effective proton energy of the present study is 14.14 MeV.

This assembly was implanted at the center of the irradiation port of the accelerator. This port is facing the analyzing magnets on the primary beam line of the accelerator. The proton beam was moved through a 6 mm diameter of the Tantalum collimator to acquire a beam of circular shape. Irradiation took place for a suitable time with 150 nA of constant current to build a sufficient activity. The number

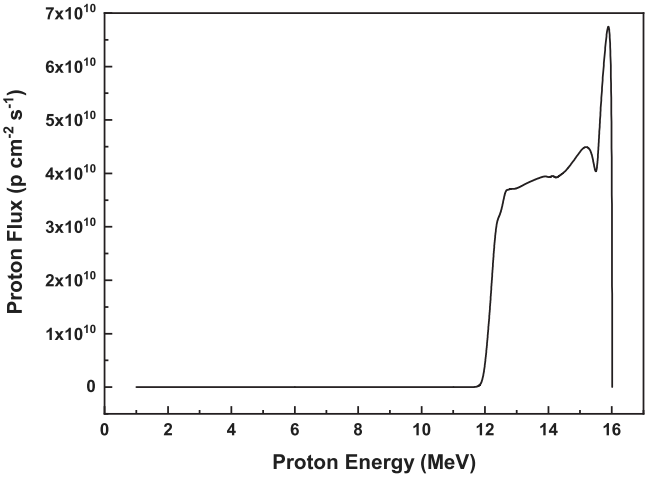

Fig. 1. Degradation in proton energy using MCNP code (ver.6.2) (Werner, 2017).

of protons targeted on the sample was calculated using current. After about eight hours of cooling, samples were taken to the pre-calibrated HPGe detector for the measurement of gamma ray energies with high resolution. The detector calibration was done using ^{152}Eu multi γ source and it was connected to a multi-channel analyzer. The collected activity of the target is shown in Fig. 2 which is in the form of γ ray spectra. The characteristic γ lines of our interest were identified by considering the respective half-lives of the resultant nuclei.

3. Data analysis

3.1. Analyzed reactions

Natural Cadmium having eight stable nuclides with atomic mass numbers A = 106, 108, 110, 111, 112, 113, 114, and 116 having isotopic abundance 1.25%, 0.89%, 12.49%, 12.80%, 24.13%, 12.22%, 28.73%, and 7.49% (nud, 2021). The ^{110}Cd nuclei with 12.49% isotopic abundance have been considered for the present study. The ^{110}In and ^{109}In radionuclides are produced via (p, n) and (p, 2n) channels, respectively. Spectroscopic details of the reactions considered for this study are given in Table 1. The ^{109}In nuclide populates in two metastable states ^{109m_1}In with half-life $T_{1/2}$ = 1.34 m and ^{109m_2}In with half-life $T_{1/2}$ = 0.209 s. Due to the shorter half-life of both metastable states, after sufficient cooling time, these states decayed by 100% IT to the ground state. Therefore, the decay of the ground state delivers the knowledge regarding total cross section production. The ^{110}In nucleus is produced in the ground state with spin $J^\pi = 7^+$ and populates in metastable state with excitation energy E_x = 62.1 keV and $J^\pi = 2^+$ spin via ^{110}Cd(p, n) reaction channel. The cross section value was evaluated for the ^{110}Cd(p, n)^{110g}In reaction corresponding to 937.478 keV of γ energy. The cross section measurement of metastable state population of ^{110}Cd(p, n) reaction is difficult as more than two reaction channel produce the product nuclei having same γ energy which is 657.75 keV, and it is difficult to separate out those reaction channels. Therefore, the theoretical model codes have been utilized for cross section estimation of ^{110}Cd(p, n)^{110m}In reaction.

3.2. Activation analysis

The standard activation technique employs for the delayed radiochemical measurement of the nuclear reactions that produced radionuclides in the same manner as in neutron activation analysis (NAA). In the activation analysis, the target gets excited by the protons and the nuclei emit characteristic γ rays. Those emitted gamma lines have a significantly long half-life and gamma ray branching intensity. Numerous

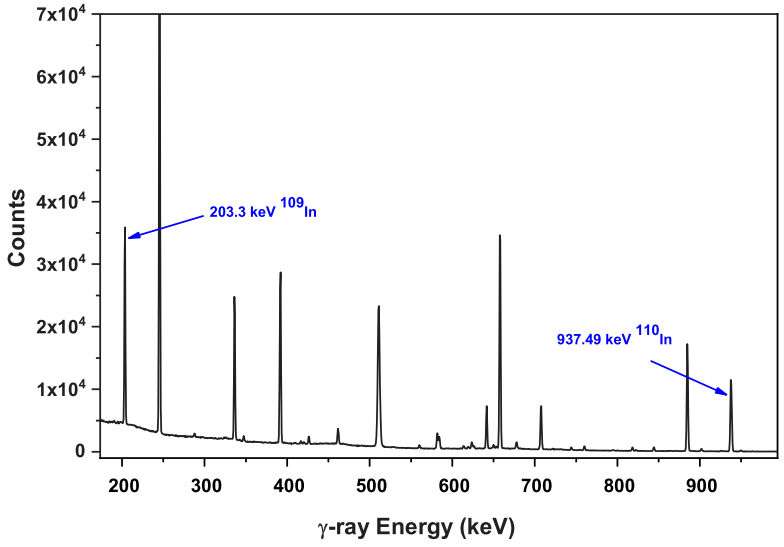

Fig. 2. Conventionally recorded γ ray spectrum using HPGe detector for irradiated ^{nat}Cd target.

Table 1
Spectroscopic data of presently studied reactions.

Reactions	Excitation energy (nud, 2021) (MeV)	Isotopic abundance (Rosman and Taylor, 1998) (%)	Threshold energy (too, 2021) (MeV)	Half-life (nud, 2021)	Decay mode (nud, 2021)	Prominent γ energy (nud, 2021) (keV)	Branching intensity (nud, 2021) (%)
^{110}Cd(p, n)^{110g}In	0.0	12.49	4.703	4.92 h (8)	ϵ = 100.00%	937.478 (13) 657.75 (10)	68.4 (19) 98 (3)
^{111}Cd(p, 2n)^{110g}In	0.0	12.80	11.472	4.92 h (8)	ϵ = 100.00%	937.478 (13) 657.75 (10)	68.4 (19) 98 (3)
^{111}Cd(p, 2n)^{110m}In	0.0	12.80	11.472	4.92 h (8)	ϵ = 100.00%	657.75 (10)	98 (3)
^{110}Cd(p, n)^{110m}In	0.0621	12.49	4.703	4.92 h (8)	ϵ = 100.00%	657.75 (5)	97.74
^{110}Cd(p, 2n)^{109g}In	0.0	12.49	12.829	4.159 (10)	ϵ = 100.00%	203.3 (1)	74.2
^{110}Cd(p, 2n)^{109m1} In	0.6501	12.49	12.829	1.34 m (7)	IT = 100.00%	649.8 (2)	93.51 (9)
^{110}Cd(p, 2n)^{109m2} In	2.1018	12.49	12.829	0.209 s (6)	IT = 100.00%	673.52 (8)	97.6 (3)

reactions may occur at high-energy charged particles so several reaction channels are available for the study (Strijckmans, 2005). The (p, d), (p, ^{3}He), (p, 2n), and (p, αn) reaction channels are crucial within 10 to 20 MeV of the proton energy range where more complex reactions will take place (Glascock, 2014).

The activation technique has been employed with gamma-ray spectroscopic analysis via off-line mode to evaluate reaction cross sections. For ^{110}Cd(p, n)^{110g}In and ^{110}Cd(p, 2n)^{109}In reactions, the cross sections have been estimated at 14.14 ± 2.03 MeV of proton energy. Table 1 contains radiation details from Nudat software (nud, 2021), while threshold energies, Q-values of the selected reactions are obtained through the Qtool (too, 2021). The γ-ray counts were collected from the spectra obtained using an HPGe detector presented in Fig. 2 for cross section measurements.

Numerous reaction channels are contributing to the same product nucleus due to natural Cadmium having eight isotopes. Therefore, it is essential to delineate the product nucleus from the merged photo peak of γ ray. The ^{110g}In radionuclide produces as a reaction product from ^{110}Cd(p, n) and ^{111}Cd(p, 2n) reaction channels and ^{109}In produces as a reaction product from ^{110}Cd(p, 2n) and ^{108}Cd(p, γ) reaction channels. For the production of ^{109}In radionuclide, the cross section contribution of ^{108}Cd(p, γ) reaction channel is very low, and in the calculation, we have corrected the count rate to remove the contribution from this reaction. Therefore, we can directly consider the cross section obtained using activation formula for ^{110}Cd(p, 2n)^{109}In reaction. The delineation of the product nuclei from the merged photo peak of γ ray was carried out for ^{110}Cd(p, n) reaction. The activity of the photo-peak of a gamma ray from ^{110}In has been delineated using the method elaborated in the literature (Smith et al., 1982; Ghosh et al., 2016; Vashi et al., 2022).

4. Nuclear model calculations

Several nuclear model codes such as TALYS, EMPIRE, ALICE, etc. are available for the identification of reaction channels and to create nuclear data libraries. These codes predict different nuclear properties in different energy ranges using various nuclear models. We have used statistical nuclear codes such as TALYS (v. 1.95), EMPIRE (v. 3.2.3), and ALICE-2014 for the simulation of nuclear data in the present study. The goal of our theoretical study with different model codes is to acquire optimum conditions for the calculations.

4.1. TALYS-1.95 code

The cross section predictions were performed with the statistical model code TALYS (v. 1.95). The code consists of various nuclear reaction models for the simulation and prediction of nuclear data for all possible channels. The code simulates nuclear reactions for light projectiles and targets heavier than Carbon for up to 200 MeV of energy. TALYS code utilizes input parameter and decay level scheme from the IAEA-RIPL data library (Capote et al., 2009b). Various nuclear models are implemented to study the impact of NLD parameters, direct, compound, pre-compound, and fission reaction mechanism for a wide energy range.

The evolution of the compound nucleus (CN) were studied by utilizing the Hauser–Feshbach approach of (Hauser and Feshbach, 1952). Also, the local potential of (Koning and Declaroche, 2003) has been utilized to study optical model potentials. The contribution of pre-equilibrium process was taken into account by using default option of exciton model (Koning and Duijvestijn, 2004). TALYS has three

Table 2
Nuclear model codes with their level density options.

Nuclear code	Level density options
TALYS-1.95	Constant Temperature + Fermi gas Model (CTM) (default) (Gilbert and Cameron, 1965) Back shifted Fermi gas Model (BFM) (Dilg et al., 1973) Generalized Superfluid Model (GSM) (Ignatyuk et al., 1979, 1993) Goriely's tables (Skyrme force) (Goriely et al., 2008) Hilaire's combinatorial tables (Skyrme force) (Goriely et al., 2008) TDHF, Hilaire's combinatorial tables (Gogny force) (Hilaire et al., 2012)
ALICE-2014	Fermi gas model (default) Back shifted pairing energies Kataria-Ramamurthy Obninsk
EMPIRE-3.2.3	EMPIRE-Specific Level Density (ESLD) (default) (Ignatyuk et al., 1975) Generalized Superfluid Model (GSM) (Gilbert and Cameron, 1965) Gilbert-Cameron Model (GCM) (Ignatyuk et al., 1979, 1993) Microscopic Hartree–Fock Bogoliubov Model (HFBM) (Goriely et al., 2008)

phenomenological models of nuclear level density and the other three options to employ microscopic approaches have been listed in Table 2. Although the calculations were performed using all the ldmodels from threshold energy to 20 MeV of proton energy, we have adopted best suitable model among them for all the reaction channels studied in the current work. For ^{110}Cd(p, n)^{110g}In reaction, the default input parameter does not reproduce data of the present measurement, and the literature data. Therefore, the input parameters have been adjusted to reproduce the acceptable cross sections. The adjustment in level density parameter was performed for the Back shifted Fermi gas Model (BFM).

By considering the energy-dependent shell effect at low energy and their loss at high energy, the level density parameter is defined below,

$$b = \tilde{b}\left[1 + \delta\epsilon_0\left(\frac{1 - e^{(-\gamma U)}}{U}\right)\right] \quad (1)$$

where,
b = level density parameter (energy dependent);
$\tilde{b}$ = asymptotic level density parameter obtained when shell effects do not exist;
γ = damping parameter determines how level density (b) differs from asymptotic level density $\tilde{b}$ at low energies;
$\delta\epsilon_0$ = shell correction energy determines dependence of level density parameter (b) on excitation energy E_x ;
$U = E_x$ - Δ = effective excitation energy;
E_x = true excitation energy ; and
Δ = pairing energy for some models that simulates odd-even effects in the nuclide.

The asymptotic value and systematic formula of damping parameter are given below,

$$\text{asymptotic value} \quad \tilde{b} = \alpha A + \beta A^{\frac{2}{3}} \quad (2)$$

$$\text{damping parameter} \quad \gamma = \frac{\gamma_1}{A^{\frac{2}{3}}} + \gamma_2 \quad (3)$$

where, α, β, $\gamma_{1,2}$ are global parameters, and A is the atomic mass of the nuclide. The default value of global parameter (α) is 0.0722. This value is adjusted using keyword "alphald" to 0.1220 which is an optimum value of BFM effective model for this reaction. The performed calculation with this adjusted parameter is plotted in Fig. 3(a), and labeled as "modified BFM".

Further, the "Rspincut" keyword was used with the modified BFM to reproduce the presently measured data, previous ones. Also, the study of the spin distribution of the excited state of CN was carried out using this keyword of TALYS. This keyword is a multiplier to the spin cut-off parameter (σ^2). The latter define the width of the angular momentum distribution of level density. It is defined as,

$$\sigma^2 = 0.01389\frac{A^{\frac{5}{4}}}{\tilde{b}}\sqrt{bU} \quad (4)$$

The symbols have their usual meanings. The spin cut-off parameter was multiplied by a factor 1.8 using the "Rspincut" keyword in TALYS (default value 1), to reproduce the suitable cross sections. The obtained data are plotted in Fig. 3(a), and labeled as "modified BFM, Rspincut = 1.8".

4.2. EMPIRE-3.2.3 code

It is widely utilized for the theoretical evaluation of nuclear reactions, and prediction of nuclear data over a broad energy range beginning with the resonance energy for neutrons to a few hundred MeV for Heavy-ion reactions (Herman et al., 2015). The code accepts light particles such as proton, neutron, deuteron (^{2}H), Triton (^{3}H), Helion (^{3}He), Helium (α), and light or heavy ions as incident particles. The input parameters like level density parameters, deformation parameters, nuclear masses, optical model parameters, gamma ray strength functions, fission barriers, and decay schemes are taken from RIPL-3 comprehensive data library (Capote et al., 2009a).

The compound nuclear reactions have been studied in the Hauser–Feshbach framework (Hauser and Feshbach, 1952). The pre-compound reaction mechanism was taken into consideration using the exciton model. The optical model parameter for outgoing proton particles was utilized. The different level densities of EMPIRE are explained by three phenomenological approach and one is based on a microscopic approach were utilized for the present calculations and mentioned them in Table 2.

Further, in order to achieve the better fit with presently measured data and EXFOR data for ^{110}Cd(p, n)^{110g}In reaction, the data were obtained using the combination of the HFBM level density model with Transition Fermi densities of Monte Carlo pre-equilibrium model (FHMS) (Blann, 1996) and MLO3 Lorentzian ver. 3 γ strength function which is plotted in Fig. 3(b).

4.3. ALICE-2014 code

The code is a theoretical nuclear model code developed using Hybrid Monte-Carlo Simulation of pre-equilibrium decay (Blann, 1971, 1996, 1972). The code accepts protons, neutrons, photons, and heavy ions, e.g. ^{4}He, and heavier elements as incident particles. The acceptable incident energy range for this code is 0.2–250 MeV. Four-level density options listed in Table 2 have been employed in the code for the cross section calculations. It is possible to change the level density and Particle Level Density (PLD) parameter of the code to obtain a considerable match of experimental measurements. The PLD can be calculated as, a_{PLD} = A/9, where, A is the atomic mass number of the composite nuclides. A study of both reactions were performed using the default level density of ALICE.

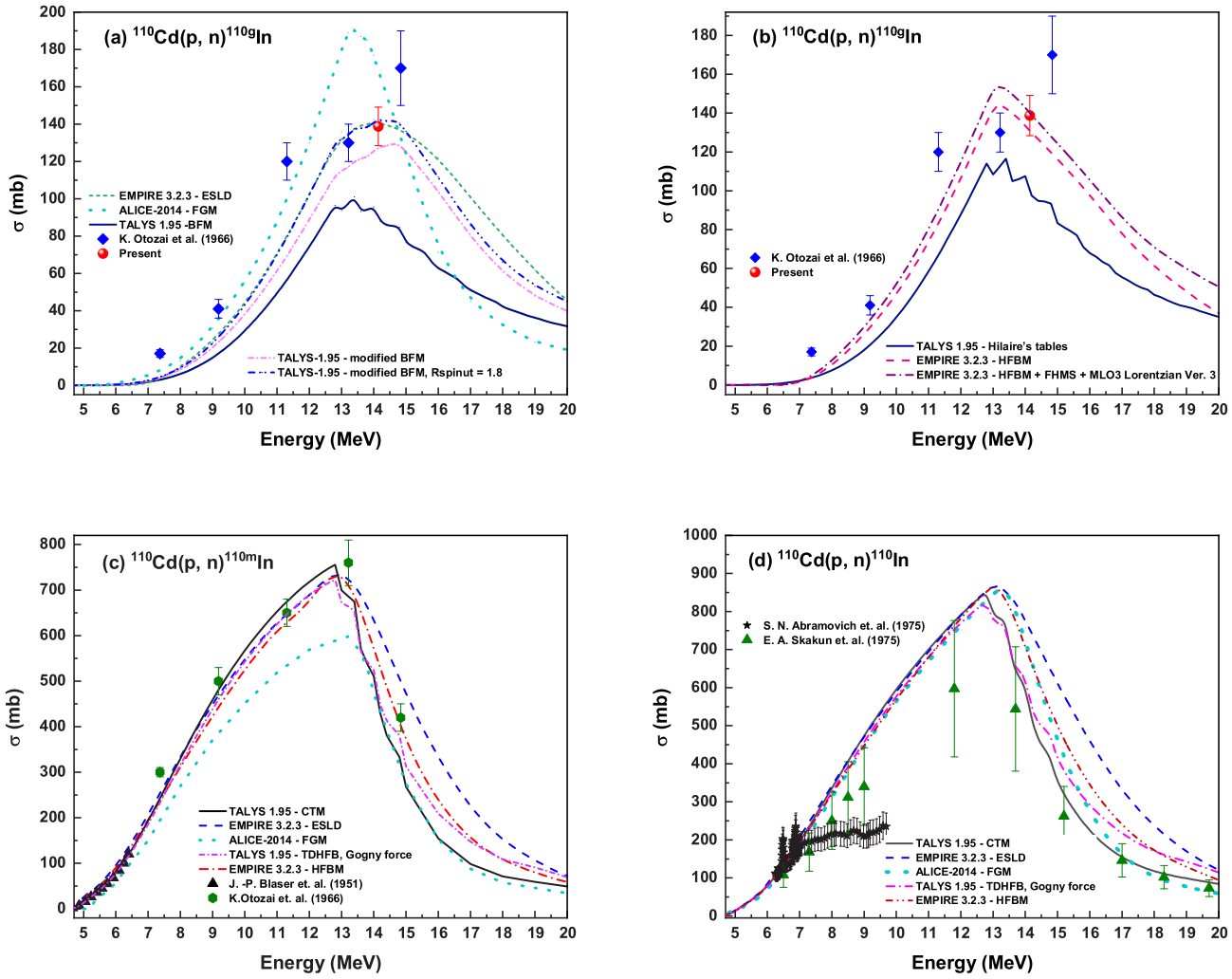

Fig. 3. Presently measured Cross section comparison of (a) ^{110}Cd(p, n)^{110g}In reaction with phenomenological models, (b) ^{110}Cd(p, n)^{110g}In reaction with microscopic models of TALYS-1.95 (Koning et al., 2017), EMPIRE-3.2.3 (Herman et al., 2015) and ALICE-2014 (Blann, 1971). The theoretical predictions of (c) ^{110}Cd(p, n)^{110m}In, and (d) ^{110}Cd(p, n)^{110}In reactions using different NLDs of TALYS-1.95, EMPIRE-3.2.3, and default NLD option of ALICE-2014, and with the EXFOR database (Zerkin and Pritychenko, 2018).

5. Results & discussion

The activation cross sections were computed for ^{110}Cd(p, n)^{110g}In and ^{110}Cd(p, 2n)^{109}In reactions at 14.14 ± 2.03 MeV of proton energy via activation method and presented in Table 3. The quadratic sum of the mentioned partial errors were considered for the uncertainty measurement in the cross section values: counting statistics (≤2%–3%), efficiency of the HPGe detector (≤3%), mass (≤0.001%), and decay parameters (≤0.5%). Further, the theoretical study has been accomplished by calculating metastable and total cross sections for ^{110}Cd(p, n)^{110}In reaction using different NLDs of TALYS and EMPIRE codes. The default model of the ALICE code has been also used in the present study.

5.1. ^{110}Cd(p, n)^{110g}In, ^{110}Cd(p, n)^{110m}In, and ^{110}Cd(p, n)^{110}In reactions

Fig. 3(a) contains the experimentally measured cross section value for ^{110}Cd(p, n)^{110g}In reaction compared with the data obtained from threshold energy (E_{th} = 4.703 MeV) to 20 MeV of proton energy using phenomenological NLD models of TALYS, EMPIRE and ALICE codes, and with the retrieved data of (Otozai et al., 1966). The estimated cross section value agrees well with the ESLD model of EMPIRE. The BFM model of TALYS predicts underestimated data than the other datasets. To overcome the discrepancy of the predicted data of TALYS, the calculations were modified by adjusting the relevant parameter set as mentioned in Section 4.1. The obtained data after modification in parameters of TALYS (i.e, modified BFM, Rspincut = 1.8) shows a better match with present measurement, predictions of the ESLD model of EMPIRE, and also with the data of K. Otozai et al. 1966. The predictions of ALICE are in good agreement with the data of K. Otozai et al. 1966 at low energy range but over-predicted than the other datasets. Over 16 MeV of proton energy, a slight variation is observed between model predictions. Due to the discrepancies in the predicted data of models at higher energies, it is essential to measure experimental data for validation of the codes that confirm the appropriateness of the model.

Fig. 3(b) shows a resemblance of presently measured experimental data with microscopic approaches of TALYS and EMPIRE predictions. Our measurement is slightly higher than the HFBM of EMPIRE-3.2.3. We have obtained theoretical data using the combination of Transition Fermi densities of Monte Carlo pre-equilibrium model (FHMS) with HFBM level densities and MLO3 modified Lorentzian ver. 3 of γ-SF which is well matched with our data. The EXFOR data is also close to the data obtained with this combination. The predictions of TALYS are lower than the present measurement, EXFOR databases, and the EMPIRE predictions.

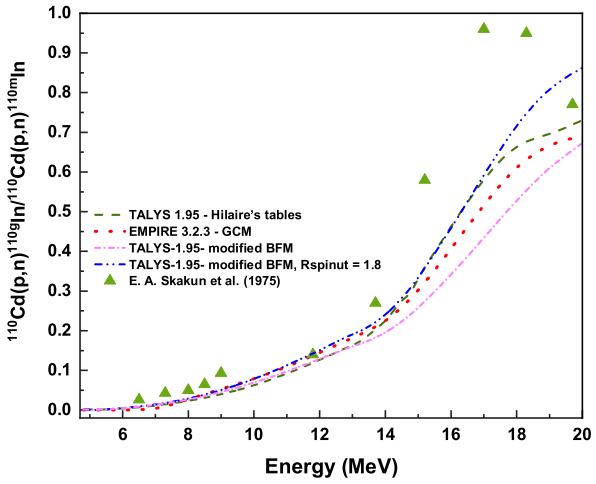

Fig. 4. The cross section ratio of the ^{110}Cd(p, n)^{110g}In (σ_g) to ^{110}Cd(p, n)^{110m}In (σ_m) reaction for the previously measured experimental data with the theoretical predictions based on the TALYS, and EMPIRE code.

Further, the comparison of default level density models of TALYS, EMPIRE, and ALICE along with the microscopic approaches such as TDHFB calculations using the Gogny force of TALYS, and HFBM model of EMPIRE with the previously reported data for ^{110}Cd(p, n)^{110m}In reaction is shown in Fig. 3(c) and for ^{110}Cd(p, n)^{110}In reaction in Fig. 3(d). It is clearly observed from Fig. 3(c) that all the level density models are compatible with one another from threshold to 14 MeV energy range except for ALICE data. For the higher energy, the data shows a slight discrepancy in the prediction. The previously reported data of (Blaser et al., 1951) covers threshold energy to 6.5 MeV of energy range and are consistent with all models' predictions. Moreover, the data of K. Otozai et al. (1966) are also consistent with all the models except ALICE-2014. Fig. 3(d) depicts that all the phenomenological and microscopic approaches of TALYS and EMPIRE predictions follow the same trend for the whole range. The data are consistent for lower energy ranges but the discrepancy has been observed for higher energy ranges. The reported data of (Abramovich et al., 1975) and (Skakun et al., 1975a) are lower than the theoretical predictions and hence cross section measurement of reactions is essential to validate codes. Also, data measurement is required to enhance the data library.

The cross section ratio adversely depends on the incident energy, spins of ground state, and metastable state. The ratio has been calculated using theoretical model codes for ^{110}Cd(p, n) reaction from threshold to 20 MeV of proton energies and presented in Fig. 4 along with the ratio retrieved from EXFOR, the existing dataset of (Skakun et al., 1975b). The ratio calculated using Hilaire's tables, the modified parameters of TALYS, and the GCM of EMPIRE has been plotted in Fig. 4. All models are well matched with the EXFOR data till 14 MeV, then the experimental data have a higher value than the predicted data.

In general, for the nuclei having higher spin than the metastable state, the ratio increases with respect to incident energy, then decreases up to some energy and remains constant for the further increase in incident energy. The increasing trend of the ratio up to certain energy range is due to the phenomenon of compound nucleus reactions. As energy increases, the pre-compound process begins, and the ratio decreases which is due to the evaporation of the low energy nucleons occur from the excited nucleus in compound nucleus process. Further, the pre-compound or non-compound reaction process initiate at higher energies in which the nucleon or nucleon clusters are emitting that removes more spin than the emission of the particle during compound nucleus process. The large angular momentum carried away by emitted high energy particles during the process. Therefore, the spin distribution of the product nuclei is commonly less than the initial spin distribution (Sateesh and Musthafa, 2012; Kim et al., 2015).

Table 3
Experimentally measured cross sections for the studied reactions.

Reactions	Energy (E_p) (MeV)	Cross section (σ) (mb)
^{110}Cd(p, n)^{110g}In	14.14 ± 2.03	139 ± 10
^{110}Cd(p, 2n)^{109}In	14.14 ± 2.03	242 ± 15

In the present case, the ground state spin (7^+) is higher than the metastable state (2^+) of the ^{110}In nuclei, that increases the probability of the ground state population with increasing energy. Fig. 4 also illustrates that the cross section ratio increases concerning the proton energy. This is the same behavior observed in the compound nuclear reaction mechanism, the higher angular momentum transferred to the CN favors the formation of high spin nuclei.

5.2. ^{110}Cd(p, 2n)^{109}In reaction

The cross section value evaluated with the activation method is presented in Fig. 5 - (a) & (b) along with theoretical predictions using different models of TALYS, EMPIRE, and default level density model of ALICE-2014 as well with the EXFOR data, MENDL-2, and TENDL-2019 evaluated data libraries.

Fig. 5(a) shows an analogy of estimated data with the phenomenological model of TALYS, EMPIRE, and ALICE. It is noticeable from the figure that experimentally measured cross section value is in the range of theoretical predictions. The earlier reported data of (Otozai et al., 1966) also match the theoretical predictions while the data of (Skakun et al., 1975a) is lower than all the level density models but nearer to the ESLD model of EMPIRE-3.2.3. As the energy increases, the discrepancy found in the data is predicted by various phenomenological models. The TENDL-2019 data and cross sections obtained using the GSM model of TALYS complement each other.

Fig. 5(b) shows an analogy of presently evaluated data with the microscopic models of TALYS and EMPIRE codes. Our data falls in the range of theoretical predictions. The data obtained from Goriely's tables of TALYS-1.95 is nearer to the previously reported data of (Otozai et al., 1966) & (Skakun et al., 1975a) retrieved from EXFOR. The cross sections of TENDL-2019 library and HFBM model of EMPIRE complement each other. The data of the MENDL-2 library is over predicted than the data predicted using all phenomenological and microscopic approaches of presently utilized codes. At the higher energies, the discrepancy in theoretical data prediction is found. Therefore, to validate the theoretical model codes, the experimental measurements are required. Moreover, the previously reported data are very ancient and scarce so new measurements using latest facilities are required.

6. Summary and conclusion

The activation cross sections have been obtained for ^{110}Cd(p, n)^{110g}In and ^{110}Cd(p, 2n)^{109}In reactions using standard activation method with γ-ray spectroscopy via off-line mode at 14.14 ± 2.03 MeV of proton energy, and simulated with the previously reported data and theoretical predictions of TALYS, EMPIRE, and ALICE. Six-NLDs of TALYS and four-NLDs of EMPIRE have been examined for the reactions. The default option (Fermi gas, PLD =9) of the ALICE-2014 code has been also used for the data simulation.

For the ^{110}Cd(p, n)^{110g}In reaction, the phenomenological BFM model of TALYS was modified with the level density and spin-cut off parameter which shows good resemblance with presently measured data, EMPIRE data, and with previously reported data of EXFOR. The combination of microscopic HFB level density with Transition Fermi densities of Monte Carlo pre-equilibrium model (FHMS), and MLO3 modified Lorentzian ver. 3 of γ-SF of EMPIRE was adopted which shows fairly good agreement with presently measured data, and EXFOR data. Also, the theoretical cross sections of metastable state population for ^{110}Cd(p,

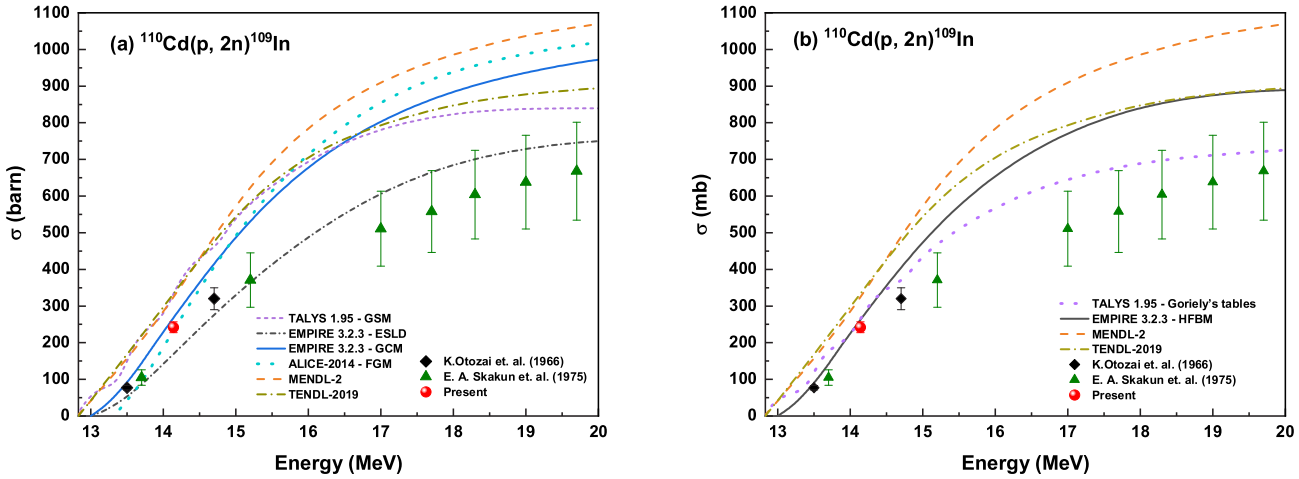

Fig. 5. Presently measured cross section comparison of (a) ^{110}Cd(p, 2n)^{109}In reaction with phenomenological models, (b) ^{110}Cd(p, 2n)^{109}In reaction with microscopic models of TALYS, EMPIRE, ALICE and with EXFOR data. The MENDL-2 and TENDL-2019 data libraries are also included.

n)^{110}In reaction were obtained using TALYS, EMPIRE, and ALICE codes, and comparison with previously reported data shows good agreement. Further, the data produced using a default model of ALICE-2014 code are under/over-predicted for the reaction. The cross section ratio (σ_g/σ_m) has been also studied theoretically for the ^{110}Cd(p, n) reaction that shows the compound nucleus mechanism. The experimentally measured cross section of ^{110}Cd(p, 2n)^{109}In reaction shows good resemblance with theoretical predictions of TALYS, EMPIRE, and ALICE. However, the data libraries MENLDL-2 and TENDL-2019 are over-predicted.

Overall, the present study observes that less experimental data are available for these reactions. Therefore, the experimental measurements are required for theoretical code validation of the studied reactions. Further, for the improvement in nuclear reactors and medical accelerators, the accurate measurement of reaction data is very important. The present study is essential for nuclear technology as Cd is used for gamma ray shielding as well as it commonly works as an obstacle to the absorption of neutrons and control of nuclear fission inside reactors. Moreover, ^{109}In and ^{110}In are also useful for the PET studies of the medical sector.

CRediT authorship contribution statement

Vibhuti Vashi: Writing – original draft, Data analysis and interpretation, Simulation, Theoretical investigation. **Rajnikant Makwana:** Conceptualization, Experiment, Visualization, Supervision, Funding acquisition, Resources, Validation, Writing – review & editing. **B. Quintana:** Supervision, Technical discussion, Review & editing. **M.H. Mehta:** Resources, Experiment, Technical discussion. **R.K. Singh:** Investigation, Experiment. **B.K. Soni:** Investigation, Experiment. **R. Chauhan:** Investigation, Experiment. **S. Mukherjee:** Resources, Technical discussion. **M. Abhangi:** Resources, Technical discussion. **S. Vala:** Resources, Technical discussion. **N.L. Singh:** Resources, Technical discussion. **G.B. Patel:** Investigation, Experiment. **S.V. Suryanarayana:** Resources, Experiment. **B.K. Nayak:** Resources, Experiment. **S.C. Sharma:** Resources, Experiment. **T.N. Nag:** Resources, Experiment. **Y. Kavun:** Supervision, Simulation support.

Declaration of competing interest

The authors declare the following financial interests/personal relationships which may be considered as potential competing interests: Rajnikant Makwana reports financial support was provided by UGC. DAE-CSR.

Data availability

Data will be made available on request

Acknowledgments

The author (RJM) acknowledges UGC-DAE Consortium for Scientific Research, Kolkata Centre for providing a research project: UGC.DAE-CSR-KC/CRS/19NPO8/0919 and to perform research work. We are thankful to the staff of BARC-TIFR Pelletron facility for the beam allotment and allowing us to use the accelerator facility. We would also like to thank Dr. G. F. Steyn from iThemba Lab of South Africa for providing ALICE-2014 calculations.

References

Brookhaven National Laboratory. Official Webpage: https://www.nndc.bnl.gov/nudat3/nudat2.jsp.
Qtool: Calculation of Reaction Q-Values and Threshold. Los Alamos National Library. http://cdfe.sinp.msu.ru/services/calc_thr/calc_thr.html.
Abramovich, S.N., et al., 1975. Izv. Rossiiskoi Akad. Nauk, Ser.Fiz. 39, 1688.
Al-Abyad, M., 2012. J. Rad. Res. Appl. Sci. 5 (2).
Al-Saleh, F.S., 2008. Radiochim. Acta 96, 461.
Alajerami, Y.S., et al., 2020. J. Appl. Phys. 127, 175102.
Alhassan, E., et al., 2020. EPJ Web Conf. 239, 13005.
Ali, B.M., et al., 2014. Nucl. Instr. Meth. Phys. Res. B 321, 30–40.
Blann, M., 1971. Phys. Rev. Lett. 27, 337.
Blann, M., 1972. Phys. Rev. Lett. 28, 757.
Blann, M., 1996. Phys. Rev. C 54, 1341.
Blaser, J.-P., et al., 1951. Helv. Phys. Acta 24, 3.
Capote, R., Herman, M., Oblozinsky, P., et al., 2009a. Ripl-reference input parameter library for calculation of nuclear reactions and nuclear data evaluations. Nucl. Data Sheets 110, 3107–3214.
Capote, R., et al., 2009b. Nucl. Data Sheets 110, 3107–3214.
Chadwik, M.B., et al., 1999. Nucl. Sci. Eng. 131, 293.
Cotton, F.A., Wilkinson, G., 1972. Zinc, Cadmium and Mercury, Advanced Inorganic Chemistry, third ed. Interscience Publishers, p. 503.
Dilg, W., Schantl, W., Vonach, H., Uhl, M., 1973. Nuclear Phys. A 217, 269.
Ditrói, F., et al., 2016. Appl. Radiat. Isot. 118, 266–276.
Eyyup TEL, et al., 2010. Pramana J. Phys. 74 (6).
Georgali, E., et al., 2020. Phys. Rev. C 102, 034610.
Ghosh, Reetuparna, et al., 2016. J. Radioanal Nucl. Chem. 307, 1481–1487.
Gilbert, A., Cameron, A.G.W., 1965. Can. J. Phys. 43, 1446.
Glascock, M.D., 2014. Treatise on Geochemistry 2nd Edition, Vol. 15. pp. 273–290.
Goriely, S., Hilaire, S., Koning, A.J., 2008. Phys. Rev. C 78, 064307.
Hauser, W., Feshbach, H., 1952. Phys. Rev. 87, 366.
Herman, M., et al., 2015. EMPIRE (Ver. 3.2.3): Nuclear Reaction Model Code System for Data Evaluation, User's Manual. INDC(NDS)-0603.
Hilaire, S., Girod, M., Goriely, S., Koning, A.J., 2012. Phys. Rev. C 86, 064317.
Ignatyuk, A.V., Smirenkin, G.N., Tishin, A.S., 1975. Sov. J. Nucl. Phys. 21 (3), 25.
Ignatyuk, A.V., et al., 1979. Sov. J. Nucl. Phys. 29 (4), 450.
Ignatyuk, A.V., et al., 1993. Phys. Rev. C 47, 1504.

Khandaker, Mayeen Uddin, et al., 2014. Nucl. Instr. Meth. Phys. Res. B 333, 80–91.
Kim, K., et al., 2015. Nuclear Phys. A 935, 65–78.
Koning, A.J., Declaroche, J.P., 2003. Nuclear Phys. A 713, 231–310.
Koning, A.J., Duijvestijn, M.C., 2004. Nuclear Phys. A 744, 15.
Koning, A.J., Hilaire, S., Goriely, S., 2017. TALYS User Manual, A Nuclear Reaction Program. NRG-1755 ZG PETTEN, The Netherlands.
Mahmoud, K.A., et al., 2020. Ceram. Int. 46 (15).
Mongelli, S.T., et al., 2005. Braz. J. Phys. 35, 894.
Otozai, K., et al., 1966. Nucl. Phys. 80, 335–348.
Patronis, N., et al., 2007. Phys. Rev. C 75, 034607.
Petti, D.A., 1989. Nucl. Technol. 84, 128.
Rios, Camilo, Méndez-Armenta, Marisela, 2019. Encyclopedia of Environmental Health, second ed. pp. 485–491.
Rosman, K.J.R., Taylor, P.D.P., 1998. Pure Appl. Chem. 70, 217.
Rubbia, C., Rubio, J.A., Buorno, S., Carminati, F., Fitier, N., Galvez, J., Gels, C., Kadi, Y., Klapisch, R., Mandrillon, P., Revol, J.P., Roche, Ch, 1995. European Organization for Nuclear Research. CERN/AT/95-44 (ET).
Sateesh, B., Musthafa, M.M., 2012. Internat. J. Modern Phys. E 21, 1250059.
Skakun, E.A., et al., 1975a. J.: Izv. Rossiiskoi Akad. Nauk, Ser. Fiz. 39, 24.
Skakun, E.A., et al., 1975b. J.ur: Izv. Rossiiskoi Akad. Nauk, Ser.Fiz. 39, 31.
Smith, D.L., et al., 1982. Nuclear Phys. A 388, 37–46.
Strijckmans, K., 2005. Encyclopedia of Analytical Science, second ed. pp. 10–20.
Tàrkànyi, F., et al., 2006. Nucl. Instr. Meth. Phys. Res. B 245, 379–394.
Vashi, Vibhuti, et al., 2022. Phy. Rev. C 105, 044613.
Werner, C.J. (Ed.), 2017. MCNP Users Manual - Code Version 6.2. Los Alamos National Laboratory, report LA-UR-17-29981.
Zerkin, V.V., Pritychenko, B., IAEA-EXFOR Experimental nuclear reaction data base, Official webpage: http://www.nds.iaea.org/exfor.